Supporting Information I

Unsymmetrical *N*-aryl-1-(pyridin-2-yl)methanimine ligands in organonickel(II) complexes – more than a blend of 2,2'-bipyridine and *N,N*-diaryl-α-diimines?

Christian Biewer[a], Claudia Hamacher[a], Andre Kaiser[a], Nicolas Vogt[a], Aaron Sandleben[a], Mason T. Chin[b], Siqi Yu[b], David A. Vicic[b], Axel Klein[a,*]

[a] Universität zu Köln, Department für Chemie, Institut für Anorganische Chemie, Greinstraße 6, D-50939 Köln, Germany

[b] Department of Chemistry, Lehigh University, 6 E. Packer Avenue, Bethlehem, Pennsylvania 18015, United States

* to whom the correspondence should be addressed: e-mail: axel.klein@uni-koeln.de

A) Experimental Section (SI)

B) ^{19}F NMR spectroscopy

C) Supporting Figures

Figure S1: ^{1}H NMR spectra of a *cis*- and *trans* [(PyMA)Ni(Mes)Br] at 293 and 213 K.

Figure S2: Crystal and molecular structure of *cis*-[(PyMA)Ni(Mes)Cl].

Figure S3: Crystal and molecular structure of 4-NO_2-PyMA.

Figure S4: Crystal and molecular structure of *trans*-[(4-NO_2-PyMA)Ni(Mes)Br].

Figure S5: Crystal and molecular structure of *cis*-[(2-CF_3-PyMA)Ni(Mes)Br].

Figure S6: Crystal and molecular structure of *cis*-[(2,4,6-Me_3-PyMA)Ni(Mes)Br].

Figure S7: Crystal and molecular structure of *cis*-[(2,6-$^{i}Pr_2$-PyMA)Ni(Mes)Br].

Figure S8: Crystal and molecular structure of *trans*-[(3,5-Me_2-PyMA)Ni(Mes)Br].

Figure S9: Powder XRD of a microcrystalline sample of [(PyMA)Ni(Mes)Br].

Figure S10: Calculated transition states during *cis-trans* isomerization of [(PyMA)Ni(Ph)Br].

Figure S11: UV-vis absorption spectrum of [(PyMA)Ni(Mes)X] in CH_2Cl_2.

Figure S12: SEC UV-vis absorption spectra of [(PyMA)Ni(Mes)Br].

Figure S13: SEC UV-vis absorption spectra of [(2-NO_2-4-Me-PyMA)Ni(Mes)Br].

D) Supporting Tables

Table S1: Selected crystal and structural refinement data for nickel complexes.

Table S2: Selected bond lengths /Å and angles /° of nickel complexes.

Table S3: Calculated energies for the *cis* and *trans* isomers of the complexes.

Table S4: Absorption maxima of the complexes [(R-PyMA)Ni(Mes)Br] in CH_2Cl_2.

Table S5: Absorptionsmaxima of [(PyMA)Ni(Mes)X] with X = F, Cl, Br, or I in various solvents.

Table S6: Selected UV-vis spectroelectrochemical data of parent and reduced complexes [(PyMA)Ni(Mes)Br], [(2-NO_2-4-Me-PyMA)Ni(Mes)Br] und [(3,5-$(OMe)_2$-PyMA)Ni(Mes)Br].

Table S7: Negishi type cross-coupling tests of [(R-PyMA)Ni(Mes)X] complexes.

A) Experimental Section

Materials. Commercially available PPh_3 (Aldrich), $NiCl_2$, $NiBr_2$ (both Chempur), MesBr, MesCl (both Acros), pyridine-2-carbaldehyde (Aldrich) and the anilines (Aldrich) were used without further purification.

Instrumentation. ^{1}H NMR spectra were recorded using Bruker Avance 300 (^{1}H: 300.13 MHz, ^{13}C: 75.47 MHz, ^{19}F: 282.35 MHz), Bruker Avance 400 (^{1}H: 400.13 MHz, ^{13}C: 100.61 MHz, ^{19}F: 376.50 MHz) using a triple resonance ^{1}H, ^{19}F, BB inverse probe head. The unambiguous assignment of the ^{1}H and ^{13}C resonances was obtained from ^{1}H NOESY, ^{1}H COSY, gradient selected ^{1}H, ^{13}C HSQC and HMBC experiments. All 2D NMR experiments were performed using standard pulse sequences from the Bruker pulse program library. Chemical shifts were relative to TMS and CCl_3F respectively. UV–vis absorption spectra were recorded with Varian Cary 05E or Cary 50 scan spectrophotometers. Elemental analyses were obtained using a HEKAtech CHNS EuroEA 3000 analyzer. EI-MS spectra were measured with a Finnigan MAT 95. Simulations were performed using ISOPRO 3.0. IR spectra were measured in ATR mode using a Perkin Elmer 400 FT-IR spectrometer. Electrochemical measurements were carried out at 100 mV/s scan rate in 0.1 M ^{n}Bu$_4$NPF$_6$ solutions using a three-electrode configuration (glassy carbon electrode, Pt counter electrode, Ag/AgCl reference) and a Metrohm Autolab PGSTAT30 potentiostat and function generator. The ferrocene/ferrocenium couple served as internal reference. Spectroelectrochemical measurements (in 0.1 M ^{n}Bu$_4$NPF$_6$ solutions) were performed using optically transparent thin-layer electrode (OTTLE) cells at ambient temperature [1] for UV-vis spectra and a two-electrode capillary for EPR studies. EPR spectra were recorded in the X band on a Bruker System ELEXSYS 500E, with a Bruker Variable Temperature Unit ER 4131VT (500 to 100 K). *g* values were calibrated using a 2,2-Diphenyl-1-picrylhydrazyl (dpph) sample.

Crystal structure analysis for 4-NO_2-PyMA ($P2_1$/n; CCDC No. 1495247), *cis*-[(PyMA)Ni(Mes)Cl] (R3c; 1495248), *trans*-[(PyMA)Ni(Mes)Br] ($P2_1$/c; 1495249), *trans*-[(4-NO_2-

PyMA)Ni(Mes)Br] ($P2_1$/n; 1495250), *trans*-[(3,5-Me_2-PyMa)Ni(Mes)Br] ($P2_1$/c; 1495251), *cis*-[(2-CF_3-PyMA)Ni(Mes)Br] ($P\bar{1}$; 1495252), *cis*-[(2-NO_2-4-Me-PyMA)Ni(Mes)Br]·CH_2Cl_2 ($P2_1$/c; 1495253), *cis*-[(2,4,6-Me_3-PyMA)Ni(Mes)Br] (C2/c; 1495254), and *cis*-[(2,6-^{i}Pr_2-PyMA)Ni(Mes)Br] ($P2_1$/c; 1495255). Crystals were obtained from concentrated CH_2Cl_2 solutions layered carefully with *n*-pentane. The data collection was performed at T = 293(2) K on a *STOE IPDS I*, *STOE IPDS II* or *STOE IPDS IIT* diffractometer all using Mo-Kα radiation (λ = 0.71073 Å) and employing ω-φ-2θ scan technique. The structures were solved by direct methods using SIR 92 [2] or SIR 2011 [3] and refinement was carried out with SHELXL 2013 employing full-matrix least-square methods on $F_0^2 \geq 2\sigma(F_0^2)$.[4] The numerical absorption corrections (X-RED V1.22; Stoe & Cie, 2001) [5] were performed after optimizing the crystal shapes using X-SHAPE V1.06 (Stoe & Cie, 1999).[6] The non-hydrogen atoms were refined with anisotropic displacement parameters without any constraints. The hydrogen atoms were included by using appropriate riding models. Details of the crystal structure solutions and refinements are summarized in Table S1 in the SI. These data can be obtained free of charge at https://summary.ccdc.cam.ac.uk/structure-summary-form or from the Cambridge Crystallographic Data Centre, 12 Union Road, Cambridge, CB2 1EZ UK (fax: +44-1223 336033 or e-mail: deposit@ccdc.cam.ac.uk).

Computational Details. Ground state electronic structure calculations on complexes [(R-PyMA)Ni(Mes)X] (X = F, Cl, Br, I) have been done on the base of density-functional theory (DFT) methods with resolution of identity coulomb approximation [7] using the TURBOMOLE [8] program packages and TMoleX 4.1 [9] user interface. For all atoms the double-ξ-valence def-SV(P) [10] and the triple-ξ-valence def2-TZVP [11] basis sets were used with *Becke's* gradient-corrected exchange-energy functional BP86.[12]

(1) Kaim, W.; Fiedler, J. Spectroelectrochemistry: the best of two worlds. *Chem. Soc. Rev.* **2009**, *38*, 3373-3382.

(2) Altomare, A.; Cascarano, G.; Giacovazzo, C.; Guagliardi, A.; Burla, M. C.; Polidori, G.; Camalli, M. *SIR-92*, A Program for Automatic Solution and Refinement of Crystal Structures, CNR Institute of Crystallography, Bari, Italy, **1994**.

(3) Burla, M. C.; Caliandro, R.; Camalli, M.; Carrozzini, B.; Cascarano, G. L.; Giacovazzo, C.; Mazzone, A.; Polidori, G.; Spagna. R. *SIR-2011*, A Program for Automatic Solution and Refinement of Crystal Structures, CNR Institute of Crystallography, Bari, Italy, **2012**.

(4) Sheldrick, G. M. *SHELXL-2013*. Program for the Refinement of Crystal Structures. University of Göttingen, Germany, **2008**.

(5) Fa. Stoe&Cie, *X-Red 1.07*, Darmstadt, **1996**.

(6) Fa. Stoe&Cie, *X-Shape 1.0.1*, Darmstadt, **1996**.

(7) Weigend, F. Accurate Coulomb-fitting basis sets for H to Rn. *Phys. Chem. Chem. Phys.* **2006**, *8*, 1057-1065.

(8) TURBOMOLE V7.0 2015, a development of University of Karlsruhe and Forschungszentrum Karlsruhe GmbH, 1989-2007, TURBOMOLE GmbH, **2007**; available from http://www.turbomole.com.

(9) Steffen, C.; Thomas, K.; Huniar, U.; Hellweg, A.; Rubner, O.; Schroer, A. TmoleX—A graphical user interface for TURBOMOLE. *J. Comput. Chem.* **2010** *31*, 2967-2970.

(10) Schäfer, A.; Horn, H.; Ahlrichs, R. Fully optimized contracted Gaussian basis sets for atoms Li to Kr. *J. Chem. Phys.* **1992**, *97*, 2571-2577.

(11) Schäfer, A.; Huber, C.; Ahlrichs, R. Fully optimized contracted Gaussian basis sets of triple zeta valence quality for atoms Li to Kr. *J. Chem. Phys.* **1994**, *100*, 5829-5835.

(12) Becke, A. D. Density-functional exchange-energy approximation with correct asymptotic behaviour. *Phys. Rev. A* **1988**, *38*, 3098-3100.

Synthesis of the *N*-aryl-1-(pyridin-2-yl)methylimine ligands (R-PyMA) - general description: To a solution of 10 mmol (1 equivalent) of the corresponding aniline in 75 mL of toluene 10 mmol (1 eq.) of pyridine-2-carbaldehyde was added in small portions. The reaction mixture was heated to reflux for about 24 h (48 h for 3,5-$(OMe)_2$-, 4-NO_2-) using a water trap. After removing the solvent under reduced pressure the products were obtained as brown oils (or yellow microcrystalline solids: 3,5-$(OMe)_2$-, 4-NO_2-, 2-NO_2-4-Me-) in 87-98% yield.

PyMA: Yield 98%. Elemental analysis found (calc. for $C_{12}H_{10}N_2$, M = 182.22 g·mol^{-1}): C 79.14 (79.10); H 5.31 (5.53); N 15.35 (15.37) %. ^{1}H NMR (300 MHz, CD_2Cl_2): 8.70 (d, 1H, H6py), 8.60 (s, 1H, =CH-), 8.23 (d, 1H, H3py), 7.83 (t, 1H, H4py), 7.46 (t, 1H, H5py), 7.39 (d, 2H, H2,6anil), 7.30 (t, 2H, H3,5anil), 7.12 (t, 1H, H4anil) ppm. EI-MS: 182 [M^+] m/z.

2,6-^{i}Pr$_2$-PyMA: Yield 94%. Elemental analysis found (calc. for $C_{18}H_{22}N_2$, M = 266.38 g·mol^{-1}): C 81.21 (81.16); H 8.31 (8.32); N 10.48 (10.52) %. ^{1}H NMR (300 MHz, $CDCl_3$): 8.74 (d, 1H, H6py), 8.31 (s, 1H, =CH-), 8.26 (d, 1H, H3py), 7.86 (t, 1H, H4Py), 7.42 (m 1H, H5py), 7.17 (m, 3H, H3,4,5anil), 2.97 (sep, 2H, ^{i}PrCH), 1.18 (d, 12H, ^{i}PrCH_3) ppm. EI-MS: 266 [M^+] m/z.

2,6-Me$_2$-PyMA: Yield 96%. Elemental analysis found (calc. for $C_{14}H_{14}N_2$, M = 210.27 g·mol^{-1}): C 79.96 (79.97); H 6.68 (6.71); N 13.36 (13.32) %. ^{1}H NMR (300 MHz, $CDCl_3$): 8.71 (d, 1H, H6py), 8.31 (s, 1H, =CH-), 8.24 (d, 1H, H3py), 7.86 (t, 1H, H4py), 7.44 (t, 1H, H5py), 7.15 (m, 3H, H3,4,5anil), 2.23 (s, 6H, $CH_3$2,6anil) ppm. EI-MS: 210 [M^+] m/z.

3,5-Me$_2$-PyMA: Yield 92 %. Elemental analysis found (calc. for $C_{14}H_{14}N_2$, M = 210.27 g·mol^{-1}): C 80.02 (79.97); H 6.75 (6.71); N 13.23 (13.32) %. ^{1}H NMR (300 MHz, CD_2Cl_2): 8.70 (d, 1H, H6py),

8.57 (s, 1H, =CH-), 8.21 (d, 1H, H3py), 7.82 (t, 1 H, H4py), 7.38 (t, 1H, H5py), 7.27 (m, 1H, H4anil), 6.94 (s, 2H, H2,6anil), 2.35 (s, 6H, $CH_3$3,5anil) ppm. EI-MS: 210 [M^+] m/z.

2,4,6-Me$_3$-PyMA: Yield 91%. Elemental analysis found (calc. for $C_{15}H_{16}N_2$, M = 224.30 g·mol^{-1}): C 80.38 (80.32); H 7.21 (7.19); N 12.40 (12.49) %. ^{1}H NMR (300 MHz, CD_2Cl_2): 8.70 (d, 1H, H6py), 8.30 (s, 1H, =CH-), 8.28 (d, 1H, H3py), 7.84 (t, 1H, H4py), 7.41 (t, 1H, H5py), 6.90 (s, 2H, H3,5anil), 2.28 (s, 3H, $CH_3$4anil), 2.12 (s, 6H, $CH_3$2,6anil) ppm. EI-MS: 224 [M^+] m/z.

3,5-(OMe)$_2$-PyMA: Yield 93%. Elemental analysis found (calc. for $C_{14}H_{14}N_2$, M = 242.27 g·mol^{-1}): C 69.56 (69.41); H 5.81 (5.82); N 11.51 (11.56) %. ^{1}H NMR (300 MHz, acetone-d^6): 8.70 (d, 1H, H6py), 8.55 (s,1H, =CH-), 8.20 (d, 1H, H3py), 7.91 (t, 1H, H4py), 7.48 (t, 1H, H5py), 6.47 (s, 2H, H2,6anil), 6.41 (t, 1H, H4anil), 3.82 (s, 6H, $OCH_3$3,5anil) ppm. EI-MS: 242 [M^+] m/z.

2-NO$_2$-4-Me-PyMA: Yield 87%. Elemental analysis found (calc. for $C_{13}H_{11}N_3O_2$, M = 241.25 g·mol^{-1}): C 64.66 (64.72); H 4.61 (4.60); N 17.47 (17.42) %. ^{1}H NMR (300 MHz, CD_2Cl_2): 8.72 (d, 1H, H6py), 8.54 (s, 1H, =CH-), 8,19 (d, 1H, H3anil), 7.88 (d, 1H, H3py), 7.76 (t, 1H, H4py), 7.44 (t, 1H, H5py), 6.96 (d, 1H, H5anil), 6.78 (d, 1H, H6anil), 2.26 (s, 3H, $CH_3$4anil) ppm. EI-MS: 241 [M+] m/z.

4-NO$_2$-PyMA: Yield 88%. Elemental analysis found (calc. for $C_{12}H_9N_3O_2$, M = 227.22 g·mol^{-1}): C 63.59 (63.43); H 3.91 (3.99); N 18.41 (18.49) %. ^{1}H NMR (300 MHz, CD_2Cl_2): 8.73 (d, 1H, H6py), 8.56 (s, 1H, =CH-), 8.29 (d, 2H, H3,5anil), 8.23 (d, 1H, H3py), 7.87 (t, 1H, H4py), 7.44 (t, 1H, H5py), 7.34 (d, 2H, H2,6anil) ppm. EI-MS: 227 [M+] m/z.

2-CF$_3$-PyMA: Yield 94%. Elemental analysis found (calc. for $C_{13}H_9F_3N_2$, M = 250.22 g·mol^{-1}): C 62.38 (62.40); H 3.71 (3.63); N 11.13 (11.20) %. ^{1}H NMR (300 MHz, CD_2Cl_2): 8.72 (d, 1H, H6py), 8.56 (s, 1H, =CH-), 8.29 (d, 1H, H3py), 7.83 (t, 1H, H4py), 7.75 (d, 1H, H3anil), 7.61 (t, 1H, H5py), 7.42-7.17 (m, 3H, H4,5,6anil) ppm. ^{19}F NMR (282 MHz, CD_2Cl_2): –59.9 (s, 3F, CF_3) ppm. EI-MS: 250 [M^+] m/z.

2-CF$_3$-6-F-PyMA: Yield 91%. Elemental analysis found (calc. for $C_{13}H_8F_4N_2$, M = 268.21 g·mol^{-1}): C 58.26 (58.22); H 3.01 (3.01); N 10.41 (10.44) %. ^{1}H NMR (300 MHz, CD_2Cl_2): 10.07 (s, 1H, =CH-), 8.80 (d, 1H, H6py), 7.96 (d, 1H, H3py), 7.88 (t, 1H, H4py), 7.53 (t, 1H, H5py), 7.28-7.17 (m, 3H, H3,4,5anil) ppm. ^{19}F NMR (282 MHz, CD_2Cl_2): –62.8 (s, 3F, 2CF_3anil); –135,0 (s, 1F, F6anil) ppm. EI-MS: 268 [M^+] m/z.

Syntheses of complexes [(R-PyMA)Ni(Mes)Br] – general description: An amount of 780 mg (1 mmol) of *trans*-[$(Ph_3P)_2$Ni(Mes)Br] were suspended in 40 mL of toluene (for Mes-PyMA and 3,5-Me_2-PyMA THF was used). Then 2 mmol (2 equivalents) of the corresponding R-PyMA ligand was added and the yellow reaction mixtures were stirred at ambient temperatures till they turned completely dark violet which took between 30 min (PyMA) and 24 h (for 2-CF_3-6-F-PyMA).

The precipitation of the products was completed by adding 40 mL of *n*-heptane. Filtration, recrystallisation from CH_2Cl_2/*n*-heptane (1:1), washing with *n*-pentane and drying under reduced pressure gave reddish violet, microcrystalline solids in 80-98% yield. Details on the yields, elemental analysis, NMR and MS were provided in the Supporting Information (SI).

***Cis/Trans*-[(PyMA)Ni(Mes)Br]:** Yield 87%. Elemental analysis found (calc. for $C_{21}H_{21}BrN_2Ni$, M = 440.00 g·mol^{-1}): C 57.36 (57.32); H 4.88 (4.81); N 6.71 (6.73) %. EI-MS: *m*/*z* = 440 $[M]^+$. *Cis/trans* (NMR) = 1.1/1. ^{1}H NMR (600 MHz, CD_2Cl_2, *cis*): 8.37 (s, 1H, =CH-), 7.98 (t, 1H, H5py), 7.66 (s, 1H, H6py), 7.47-7.32 (m, 4H, H3py, H2,6anil, H4anil), 7.33 (t, 1H, H4py), 6.99 (t, 2H, H3,5anil), 6.48 (s, 2H, H3,5Mes), 2.96 (s, 6H, $CH_3$2,6Mes), 2.19 (s, 3H, $CH_3$4Mes) ppm.

^{1}H NMR (600 MHz, CD_2Cl_2, *trans*): 9.38 (d, 1H, H6py), 8.31 (s, 1H, =CH-), 8.02 (t, 1H, H4py), 7.74 (t, 1H, H5py), 7.72-7.32 (m, 3H, H3py, H2,6anil), 7.04 (t, 1H, H4anil), 6.74 (t, 2H, H3,5anil), 6.11 (s, 2H, H3,5Mes), 2.86 (s, 6H, $CH_3$2,6Mes), 1.95 (s, 3H, $CH_3$4Mes).

***Cis/Trans*-[(3,5-Me$_2$-PyMA)Ni(Mes)Br]:** Yield 98%. Elemental analysis found (calc. for $C_{23}H_{25}N_2Ni_1Br_1$, M = 468.06 g·mol^{-1}): C 59.06 (59.02); H 5.31 (5.38); N 5.97 (5.99) %. EI-MS: *m*/*z* = 468 $[M]^+$. *Cis/trans* (NMR) = 1.5/1. ^{1}H NMR (400 MHz, CD_2Cl_2, *cis*): 8.71 (s, 1H, =CH-), 8.32 (t, 1H, H5py), 8.24 (d, 1H, H6py), 8.05 (m, 1H, H4py), 7.85 (d, 1H, H3py), 7.05 (s, 2H, H2,6anil), 6.73 (s, 1H, H4anil), 6.33 (s, 2H, H3,5Mes), 3.05, (s, 3H, $CH_3$4Mes), 2.95 (s, 6H, $CH_3$2,6Mes), 2.09 (s, 6H, $CH_3$2,6anil) ppm. ^{1}H NMR (400 MHz, CD_2Cl_2, *trans*): 9,51 (d, 1H, H6py), 8,60 (s, 1H, =CH-), 8.41 (t, 1H, H4py), 8.05 (m, 2H, H5py), 7.64 (d, 1H, H3py), 7,74 (s, 2H, H2,6anil), 6.94 (s, 1H, H4anil), 6.21 (s, 2H, H3,5Mes), 2.42 (s, 6H, $CH_3$2,6Mes), 2.29 (s, 3H, $CH_3$4Mes), 1,31 (s, 6H, $CH_3$2,6anil) ppm.

***Cis*-[(2,4,6-Me$_3$-PyMA)Ni(Mes)Br]:** Yield 82%. Elemental analysis found (calc. for $C_{24}H_{27}N_2Ni_1Br_1$, M = 482.08 g·mol^{-1}): C 59.76 (59.79); H 5.31 (5.35); N 5.87 (5.81) %. EI-MS: *m*/*z* = 482 $[M]^+$. ^{1}H NMR (400 MHz, CD_2Cl_2): 8.19 (s, 1H, =CH-), 7.99 (t, 1H, H5py), 7.60 (d, 1H, H6py), 7.38 (t, 1H, H4py), 7.34 (d, 1H, H3py), 6.94 (s, 2H, H3,5anil), 6.52 (s, 2H, H3,5Mes), 2.98 (s, 6H, $CH_3$2,6Mes), 2.40 (s, 6H, $CH_3$2,6anil), 2.32 (s, 3H, $CH_3$4anil), 2.23 (s, 3H, $CH_3$4Mes) ppm.

***Cis*-[(2,6-^{i}Pr$_2$-PyMA)Ni(Mes)Br]:** Yield 77%. Elemental analysis found (calculated for $C_{27}H_{33}N_2NiBr$, M = 524.16 g·mol^{-1}): C 61.86 (61.87); H 6.33 (6.35); N 5.32 (5.34) %. EI-MS: *m*/*z* = 524 $[M]^+$. ^{1}H NMR (300 MHz, CD_2Cl_2): 8.20 (s, 1H, =CH-), 8.01 (m, 1H, H5py), 7.62 (d, 1H, H6py), 7.40 (m, 1H, H4py), 7.37 (m, 1H, H3py), 7.20 (m, 3H, H3,4,5anil), 6.53 (s, 2H, H3,5Mes), 3.51 (sep, 2H, ^{i}Pr-CH), 2.96 (s, 6H, $CH_3$2,6Mes), 2.24 (s, 3H, $CH_3$4Mes), 1.47 (d, 6H, ^{i}Pr-CH_3-*endo*), 1.16 (d, 6H, ^{i}Pr-CH_3-*exo*) ppm.

***Cis*-[(2,6-Me$_2$-PyMA)Ni(Mes)Br]:** Yield 87%. Elemental analysis found (calculated) (for $C_{23}H_{25}N_2NiBr$, M = 468.06 g·mol^{-1}): C 59.09 (59.02); H 5.40 (5.38); N 6.02 (5.99) %. EI-MS: *m*/*z* = 468 $[M]^+$. ^{1}H NMR (300 MHz, CD_2Cl_2): 8.21 (s, 1H, =CH-), 8.00 (t, 1H, H5py), 7.61 (d, 1H,

H6py), 7.38 (m, 2H, H4,3py), 7.12 (m, 3H, H3,4,5anil), 6.52 (s, 2H, H3,5Mes), 2.99 (s, 6H, $CH_3$2,6Mes), 2.44 (s, 6H, $CH_3$2,6anil), 2.24 (s, 3H, $CH_3$4Mes) ppm.

***Cis/Trans*-[(3,5-(OMe)$_2$-PyMA)Ni(Mes)Br]:** Yield 89%. Elemental analysis found (calculated) (for $C_{23}H_{25}N_2NiBrO_2$, M = 500.05 g·mol^{-1}): C 55.19 (55.24); H 5.40 (5.44); N 5.62 (5.60)%. EI-MS: *m*/*z* = 500 [M]$^+$. *Cis/trans* (NMR) = 1.41/1. ^{1}H NMR (300 MHz, CD_2Cl_2, *cis*): 8.61 (s, 1H, =CH-), 8.39 (t, 1H, H5py), 8.06 (m, 1H, H6py), 7.86 (t, 1H, H4py), 7.78 (m, 1H, 3py), 7.37 (s, 2H, H2,6anil), 6.61 (s, 1H, H4anil), 6.25 (s, 2H, H3,5Mes), 3.89 (s, 6H, $OCH_3$3,5anil), 3.05 (s, 6H, $CH_3$2,6Mes), 2.23 (s, 3H, $CH_3$4Mes) ppm. ^{1}H NMR (300 MHz, CD_2Cl_2, *trans*): 9.53 (d, 1H, H6py), 8.45 (s, 1H, =CH-), 8.73 (t, 1H, H4py), 8.06 (m, 1H, H5py), 7.78 (m, 1H, H3py), 7.37 (s, 2H, H2,6anil), 6.56 (s, 1H, H4anil), 5.95 (s, 2H, H2,6Mes), 3.66 (s, 6H, $OCH_3$3,5anil), 2.99 (s, 6H, $CH_3$2,6Mes), 2.11 (s, 3H, $CH_3$4Mes) ppm.

***Cis*-[(2-NO$_2$-4-Me-PyMA)Ni(Mes)Br]:** Yield 80%. Elemental analysis found (calculated) (for $C_{22}H_{22}N_3NiBrO_2$, M = 499.03 g·mol^{-1}): C 52.99 (52.95); H 4.40 (4.44); N 8.42 (8.42) %. EI-MS: *m*/*z* = 499 [M]$^+$. ^{1}H NMR (300 MHz, CD_2Cl_2): 8.46 (s, 1H, =CH-), 8.05 (m, 2H, H5py, H3anil), 7.75 (d, 1H, H6py), 7.61 (d, 1H, H6anil), 7.43 (m, 2H, H4py, H5anil), 7.13 (d, 1H, H3py), 6.53 (s, 2H, H3,5Mes), 2.83 (s, 6H, $CH_3$2,6Mes), 2.53 (s, 3H, $CH_3$4anil), 2.06 (s, 3H, $CH_3$4Mes) ppm.

***Cis/Trans*-[(4-NO$_2$-PyMA)Ni(Mes)Br]:** Yield 95%. Elemental analysis found (calculated) (for $C_{21}H_{20}N_3NiBrO_2$, M = 485.01 g·mol^{-1}): C 51.99 (52.01); H 4.20 (4.16); N 8.62 (8.66) %. EI-MS: *m*/*z* = 483 [M]$^+$. *Cis:trans* (NMR) = 1.1/1. ^{1}H (400 MHz, CD_2Cl_2, *cis*): 8.58 (s, 1H, =CH-), 8.10 (m, 1H, H5py), 7.87 (m, 3H, H6py, H4py, H3py), 7.76 (d, 2H, H2,6anil), 7.44 (d, 2H, H3,5anil), 6.56 (s, 2H, H3,5Mes), 3.02 (s, 6H, $CH_3$2,6Mes), 2.30 (s, 3H, $CH_3$4Mes) ppm. ^{1}H NMR (400 MHz, CD_2Cl_2, *trans*): 9.58 (d, 1H, H6py), 8.48 (s, 1H, =CH-), 8.35 (t, 1H, H4py), 8.10 (m, 1H, H5py), 7.87 (m, 1H, H3py), 7.59 (d, 2H, H2,6anil), 6.94 (d, 2H, H3,5anil), 6.20 (s, 2H, H3,5Mes), 2.93 (s, 6H, $CH_3$2,6Mes), 2.06 (s, 3H, $CH_3$4Mes) ppm.

***Cis*-[(2-CF$_3$-PyMA)Ni(Mes)Br]:** Yield 94%. Elemental analysis found (calculated) (for $C_{22}H_{20}N_2NiBrF_3$, M = 508.01 g·mol^{-1}): C 52.05 (52.02); H 3.98 (3.97); N 5.52 (5.51) %. EI-MS: *m*/*z* = 506 [M]$^+$. ^{1}H NMR (300 MHz, CD_2Cl_2): 8.40 (s, 1H, =CH-), 8.05 (t, 1H, H5py), 7.80 (d, 1H, H6py), 7.71 (m, 2H, H3py, H4py), 7.54-7.37 (m, 4H, H3,4,5,6anil), 6.55 (s, 2H, H3,5Mes), 3.03 (s, 6H, $CH_3$2,6Mes), 2.27 (s, 3H, $CH_3$4Mes) ppm. ^{19}F NMR (282 MHz, CD_2Cl_2): –57.1 (s, 3F, $CF_3$2anil) ppm.

***Cis*-[(2-CF$_3$-6-F-PyMA)Ni(Mes)Br]:** Yield 91%. Elemental analysis found (calculated) (for $C_{22}H_{19}N_2NiBrF_4$, M = 526.00 g·mol^{-1}): C 50.29 (50.24); H 3.68 (3.64); N 5.42 (5.33) %. EI-MS: *m*/*z* = 524 [M]$^+$. ^{1}H NMR (300 MHz, acetone-d^6): 8.45 (s, 1H, =CH-), 8.03 (t, 1H, H5py), 7.71 (d, 1H, H6py), 7.56 (t, 1H, H4py), 7.44 (m 4H, H3py, H3,4,5anil), 6.52 (s, 2H, H3,5Mes), 2.94 (s, 6H,

$CH_3$2,6Mes), 2.24 (s, 3H, $CH_3$4Mes) ppm. ^{19}F NMR (282 MHz, acetone-d^6): –57.6 (s, 3F, $CF_3$2anil), –119.0 (s, 1F, F6anil) ppm.

Syntheses of c*is/trans*-[(PyMA)Ni(Mes)Cl]: An amount of 0.737 g (1 mmol) of *trans*-[$(Ph_3P)_2$Ni(Mes)Cl] was suspended in 40 mL of toluene and 365 mg (2 mmol) of PyMA were added. After stirring for 30 min the reaction mixture had turned from yellow to dark violet and vast portions of the products precipitated. Addition of 40 mL of *n*-heptane lead to complete precipitation and supernatant solvent was decanted. The dark violet residue was washed thrice with 20 mL of *n*-pentane and dried under reduced pressure. Yield: 325 mg, 0.82 mmol, 82%. Elemental analysis found (calculated) (for $C_{21}H_{21}N_2NiCl$, M = 395.56 g·mol^{-1}): C 63.59 (63.77); H 5.28 (5.35); N 7.02 (7.08) %. EI-MS: *m*/*z* = 394 [M]$^+$. *Cis/trans* (NMR) = 1.25/1. ^{1}H NMR (300 MHz, CD_2Cl_2, *cis*): 8.33 (s, 1H, =CH-), 7.91 (t, 1H, H5py), 7.59 (s, 1H, H6py), 7.43-7.32 (m, 4H, H3py, H2,4,6anil), 7.30 (t, 1H, H4py), 7.04 (t, 2H, 3,5anil), 6.45 (s, 2H, H3,5Mes), 2.96 (s, 6H, $CH_3$2,6Mes), 2.20 (s, 3H, $CH_3$4Mes) ppm. ^{1}H NMR (300 MHz, CD_2Cl_2, *trans*): 9.33 (d, 1H, H6py), 8.32 (s, 1H, =CH-), 7.99 (t, 1H, H4py), 7.70 (t, 1H, H5py), 7.73-7.30 (m, 3H, H3py, H2,6anil), 7.11 (t, 1H, H4anil), 6.73 (t, 2H, H3,5anil), 6.08 (s, 2H, H3,5Mes), 2.81 (s, 6H, $CH_3$2,6Mes), 1.94 (s, 3H, $CH_3$4Mes).

For long-time storage these complexes have to be protected from humidity. From elemental analyses and ^{1}H NMR and ^{19}F spectroscopies, the entity and high purity of the obtained materials is evident (details in the Experimental Section). The stability of the [(R-PyMA)Ni(Mes)X] complexes in solution resemble very much to the bpy and related derivatives studied previously.[13-16] In carefully dried non-coordinating and non-protic solvents such as THF, CH_2Cl_2, toluene or acetone the complexes are stable for days. Coordinating solvents such as DMF and acetonitrile rapidly cleave the halide ligand within minutes, followed by a slower cleavage of the PyMA ligands taking days. Water contaminated coordinating solvents and protic solvents such as methanol or ethanol lead to decomposition of the complexes within a day, leaving the uncoordinated ligand and greenish material presumably containing octahedral Ni(II) aqua complexes.[13]

(13) Feth, M. P.; Klein, A.; Bertagnolli, H. Investigation of the Ligand Exchange Behavior of Square-Planar Nickel (II) Complexes by X-ray Absorption Spectroscopy and X-ray Diffraction. *Eur. J. Inorg. Chem*. **2003**, 839-852.
(14) Klein, A.; Kaiser, A.; Wielandt, W.; Belaj, F.; Wendel, E.; Bertagnolli, H.; Zalis, S. Halide Ligands: More Than Just σ-Donors? A Structural and Spectroscopic Study of Homologous Organonickel Complexes. *Inorg. Chem.* **2008**, *47*, 11324-11333.

(15) Feth, M. P.; Klein, A.; Bertagnolli, H.; Záliš, S. On the Electronic Structure of Mesitylnickel Complexes of α-Diimines – Combining Structural Data, Spectroscopy and Calculations. *Eur. J. Inorg. Chem*. **2004**, 2784-2796.
(16) Klein, A.; Schmieder, A.-K.; Hurkes, N.; Hamacher, C.; Schüren, A. O.; Feth, M. P.; Bertagnolli, H. Mono-and Binuclear Arylnickel Complexes of the α-Diimine Bridging Ligand 2, 2′-Bipyrimidine (bpym). *Eur. J. Inorg. Chem.* **2010**, 934-941.

Catalytic Negishi Cross-Coupling Reactions. 0.5 mL pentylzinc bromide, or 2-(1,3-dioxolan-2-yl)]ethyl]zinc bromide solution in THF (0.25 mmol), 0.012 mmol of nickel catalyst, and 55 mg (0.25 mmol) of 4-iodotoluene were added to 15 mL of THF. The solution was stirred for 12 hours and then quenched with water. The organic layer was collected and passed through a small alumina plug using methanol as the eluent. The yields were calculated by GC using hexamethylbenzene as a calibrated internal standard.

B) ^{19}F NMR spectroscopy.

The fluoride co-ligand in the *cis* and *trans* isomers of [(PyMA)Ni(Mes)F] reveal a ^{19}F NMR signal at –252 and –275 ppm, respectively, reflecting the geometric differences. Recently, we reported for the bpy derivative [(bpy)Ni(Mes)F] a value of –407 ppm (referenced vs. $CFCl_3$).[14] This value calculates to –330 ppm vs. CF_3COOH and is fully in line with reported values ranging from –330 to –390 ppm for square planar Ni–F complexes with perfluorinated aryl ligands *trans* to F and phosphines or carbenes in the two lateral positions.[17-21] Also in the complex *cis*-[(dippe)Ni(C_6F_4H-2)F] (dippe = 1,2-bis(diisopropyl)phosphino-ethane) with a phosphine *trans* to F the value lies in the same range (–345 ppm).[22] The relatively low-field shifted values for the two [(PyMA)Ni(Mes)F] complexes might be due to the pronounced π-accepting nature of the PyMA ligand lowering the overall electron density in the F ligand.

(17) Hatnean, J. A.; Shoshani, M.; Johnson, S. A. Mechanistic insight into carbon–fluorine cleavage with a (iPr$_3$P)$_2$Ni source: Characterization of (iPr$_3$P)$_2$NiC_6F_5 as a significant Ni(I) byproduct in the activation of C_6F_6. *Inorg. Chim. Acta* **2014**, *422*, 86-94.
(18) Fischer, P.; Götz, K.; Eichhorn, A.; Radius, U. Decisive Steps of the Hydrodefluorination of Fluoroaromatics using [Ni(NHC)$_2$]. *Organometallics* **2012**, *31*, 1374-1383.
(19) Steffen, A.; Sladek, M. I.; Braun, T.; Neumann, B.; Stammler, H.-G. Catalytic C−C Coupling Reactions at Nickel by C−F Activation of a Pyrimidine in the Presence of a C−Cl Bond: The Crucial Role of Highly Reactive Fluoro Complexes. *Organometallics* **2005**, *24*, 4057-4064.

(20) Burling, S.; Elliott, P. I. P.; Jasim, N. A.; Lindup, R. J.; McKenna, J.; Perutz, R. N.; Archibald, S. J.; Whitwood, A. C. C–F Bond activation at Ni (0) and simple reactions of square planar Ni (II) fluoride complexes. *Dalton Trans.* **2005**, 3686-3695.

(21) Braun, T.; Perutz, R. N. Routes to fluorinated organic derivatives by nickel mediated C–F activation of heteroaromatics. *Chem. Commun.* **2002**, 2749-2757.

(22) Arevalo, A.; Tlahuext-Aca, A.; Flores-Alamo, M.; Garcia, J. J. On the catalytic hydrodefluorination of fluoroaromatics using nickel complexes: the true role of the phosphine. *J. Am. Chem. Soc.* **2014**, *136*, 4634-4639.

C) Supporting Figures

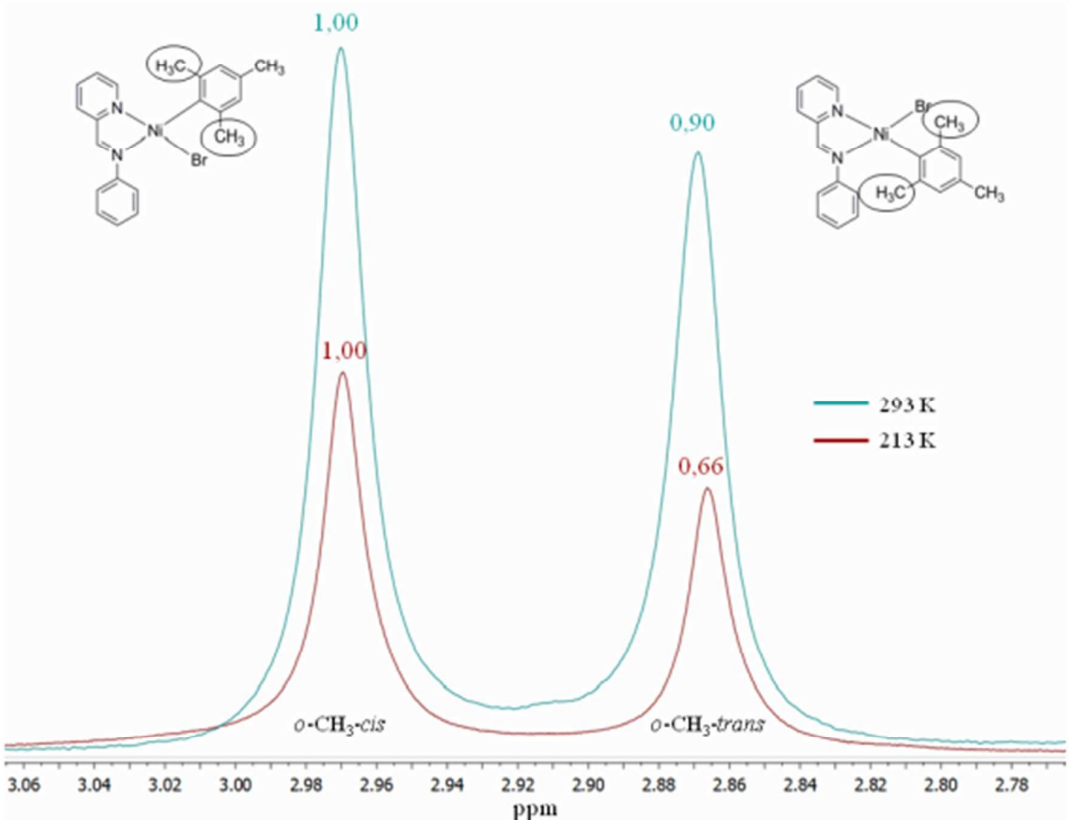

Figure S1: ^{1}H NMR spectra of a *cis*- and *trans* isomeric mixture of [(PyMA)Ni(Mes)Br] in CD_2Cl_2 at 293 (blue) and 213 (red) K.

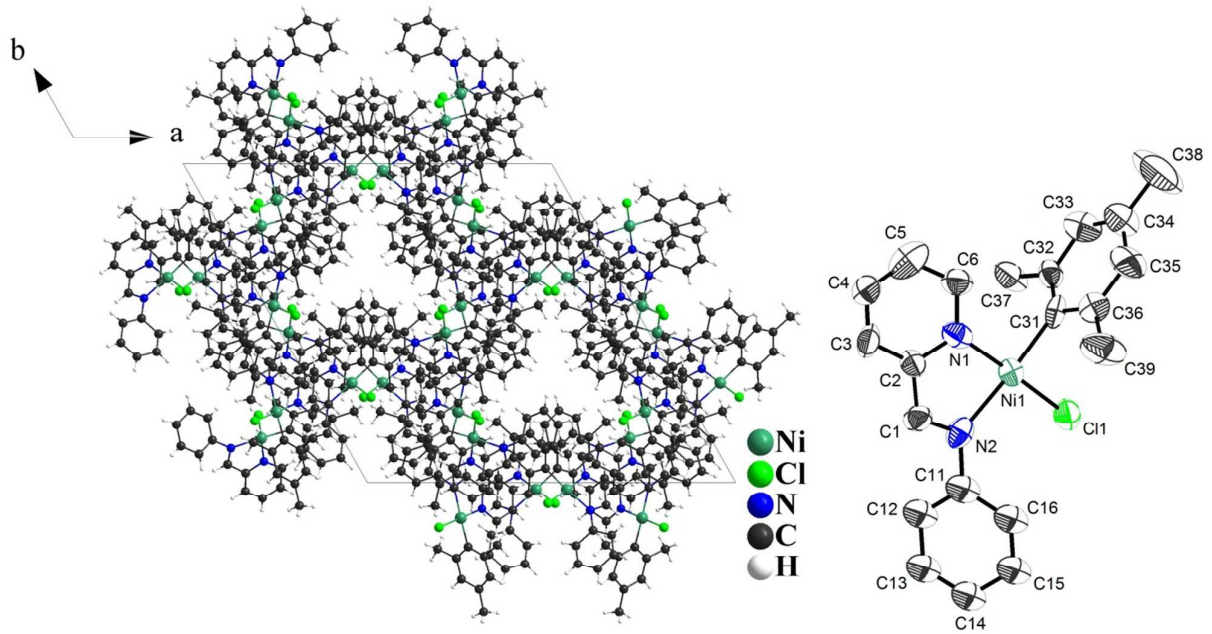

Figure S2: To the left: Crystal structure of *cis*-[(PyMA)Ni(Mes)Cl]. (viewed along the crystallographic *c* axis). To the right: Molecular structure (thermal ellipsoids at 50% probability level), H atoms are omitted for clarity.

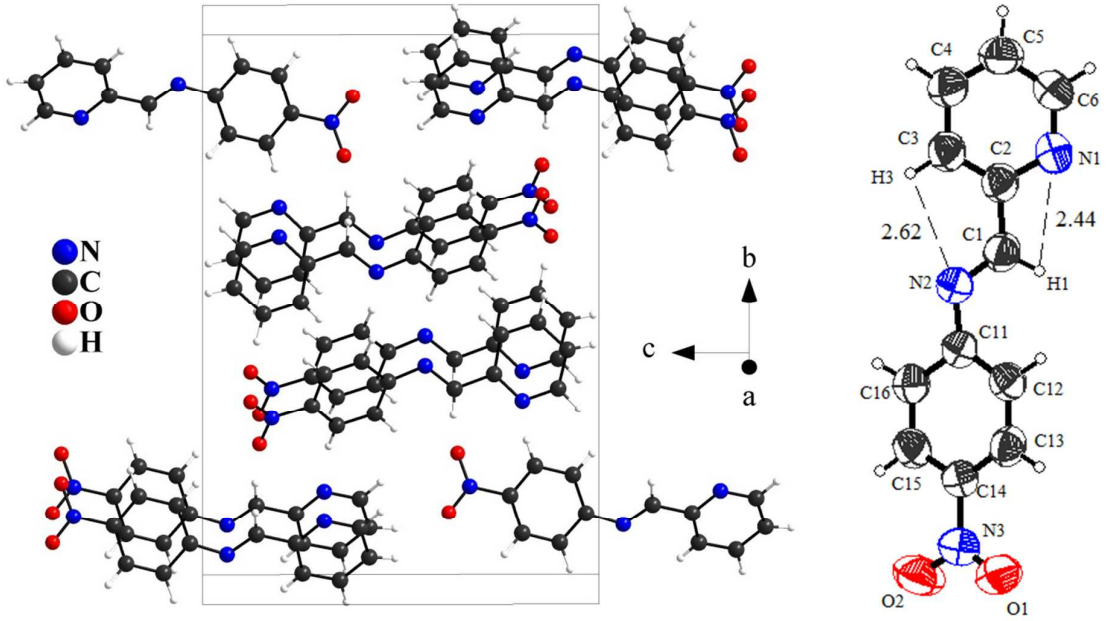

Figure S3: To the left: Crystal structure of 4-NO_2-PyMA. To the right: Molecular structure (thermal ellipsoids at 50% probability level) showing also the intramolecular C–H···N bond).

The ligand 4-NO_2-PyMA was refined in the space group $P2_1/n$ and exhibits no intermolecular interactions in the crystal. The molecular structure (Figure S7) shows an *N,N-trans* configuration,

supported by two C–H···N hydrogen bridges and a coplanar N=CH–Py unit. The aniline core with an almost coplanar NO_2 group (~5°) exhibits a ~45° dihedral angle to the N=CH–Py plane.

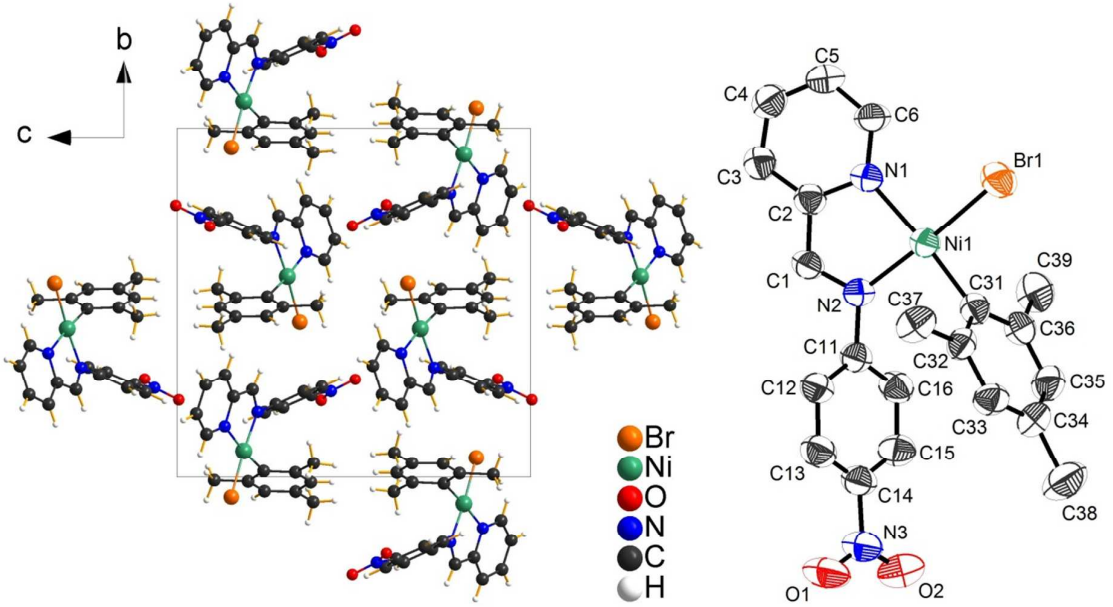

Figure S4: To the left: Crystal structure of *trans*-[(4-NO_2-PyMA)Ni(Mes)Br] (viewed along the crystallographic *a* axis). To the right: Molecular structure (thermal ellipsoids at 50% probability level, H atoms are omitted for clarity).

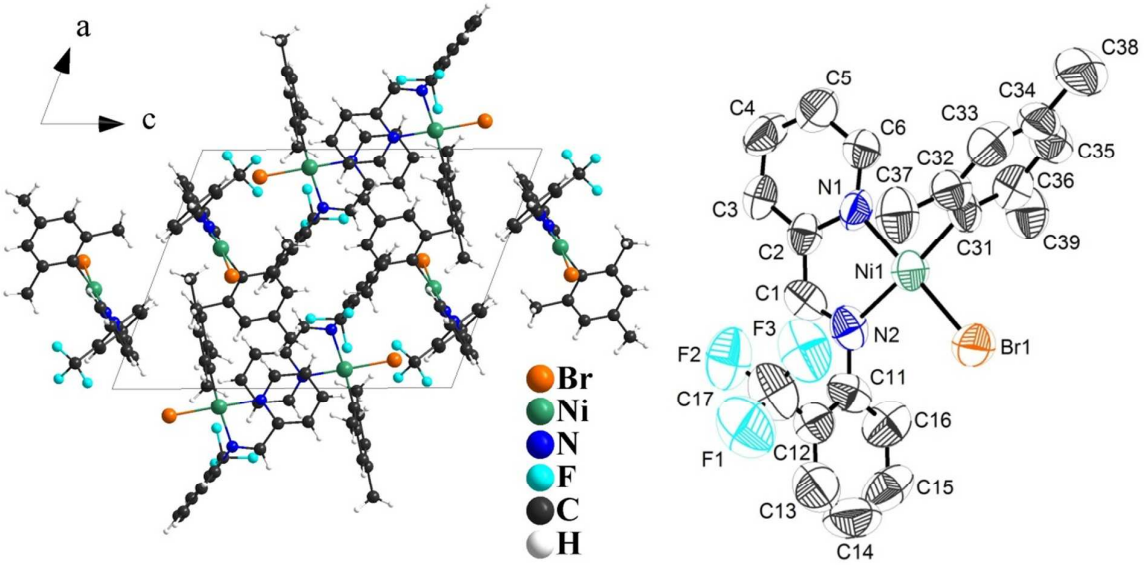

Figure S5: To the left: Crystal structure of *cis*-[(2-CF_3-PyMA)Ni(Mes)Br] (viewed along the crystallographic *b* axis). To the right: Molecular structure of one of two crystallographic independent molecules (thermal ellipsoids at 50% probability level), H atoms are omitted for clarity.

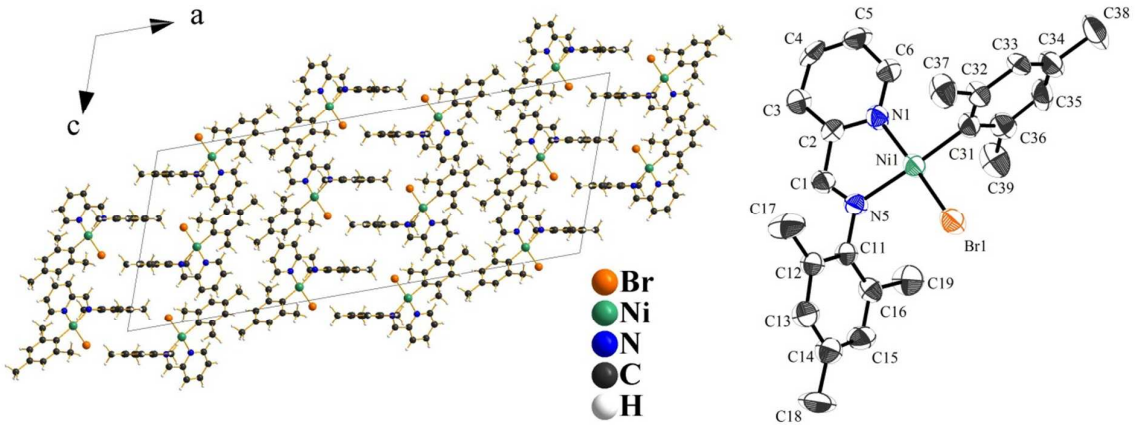

Figure S6: To the left: Crystal structure of *cis*-[(2,4,6-Me_3-PyMA)Ni(Mes)Br] (viewed along the crystallographic *b* axis). To the right: Molecular structure (thermal ellipsoids at 50% probability level, H atoms are omitted for clarity).

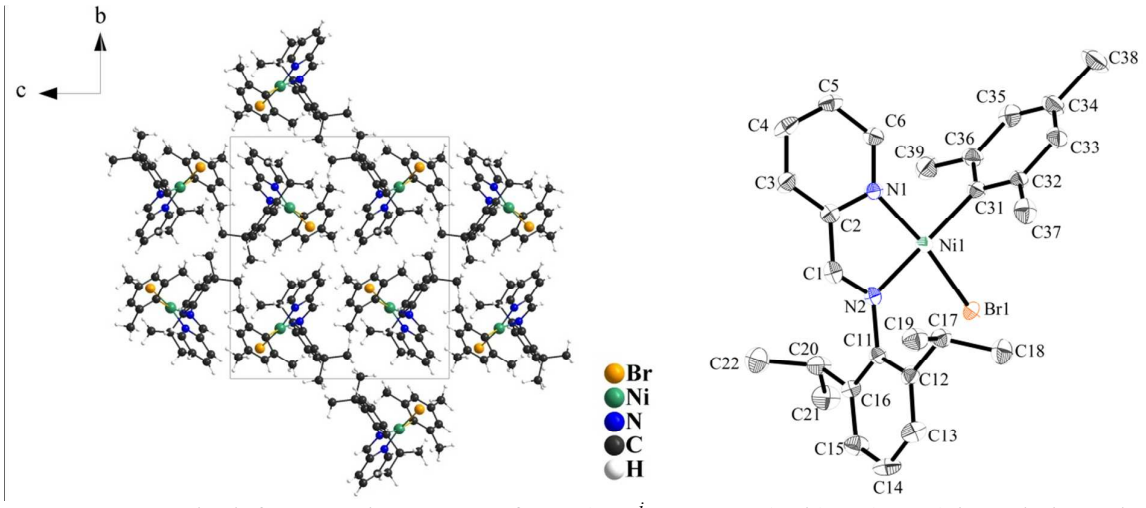

Figure S7: To the left: Crystal structure of *cis*-[(2,6-$^{i}Pr_2$-PyMA)Ni(Mes)Br] (viewed along the crystallographic *a* axis). To the right: Molecular structure (thermal ellipsoids at 50% probability level), H atoms are omitted for clarity.

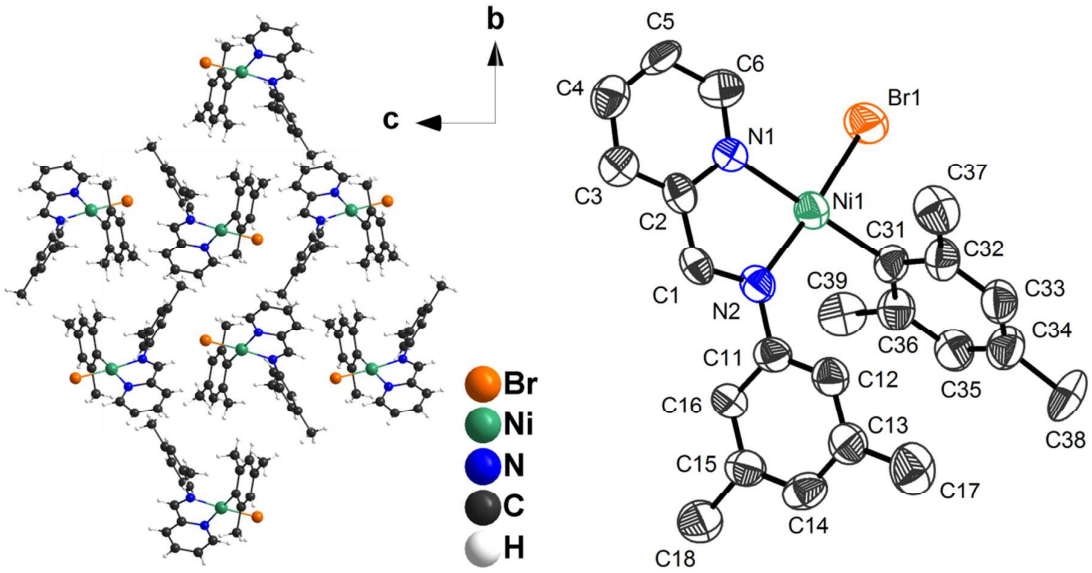

Figure S8: To the left: Crystal structure of *trans*-[(3,5-Me_2-PyMA)Ni(Mes)Br] (viewed along the crystallographic *a* axis). To the right: Molecular structure (thermal ellipsoids at 50% probability level), H atoms are omitted for clarity.

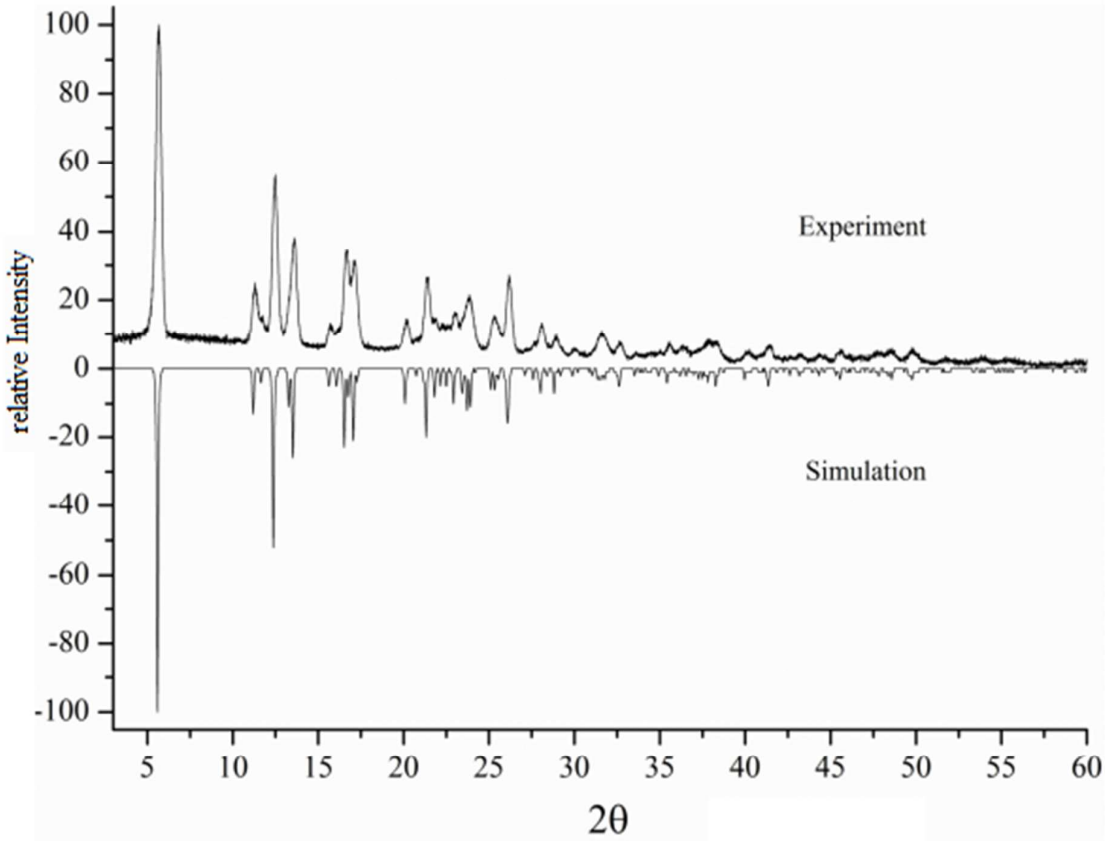

Figure S9: Powder XRD of a microcrystalline sample of [(PyMA)Ni(Mes)Br] (Experiment) compared with the calculated 2θ plot of the crystallized *trans*-[(PyMA)Ni(Mes)Br] (Simulation).

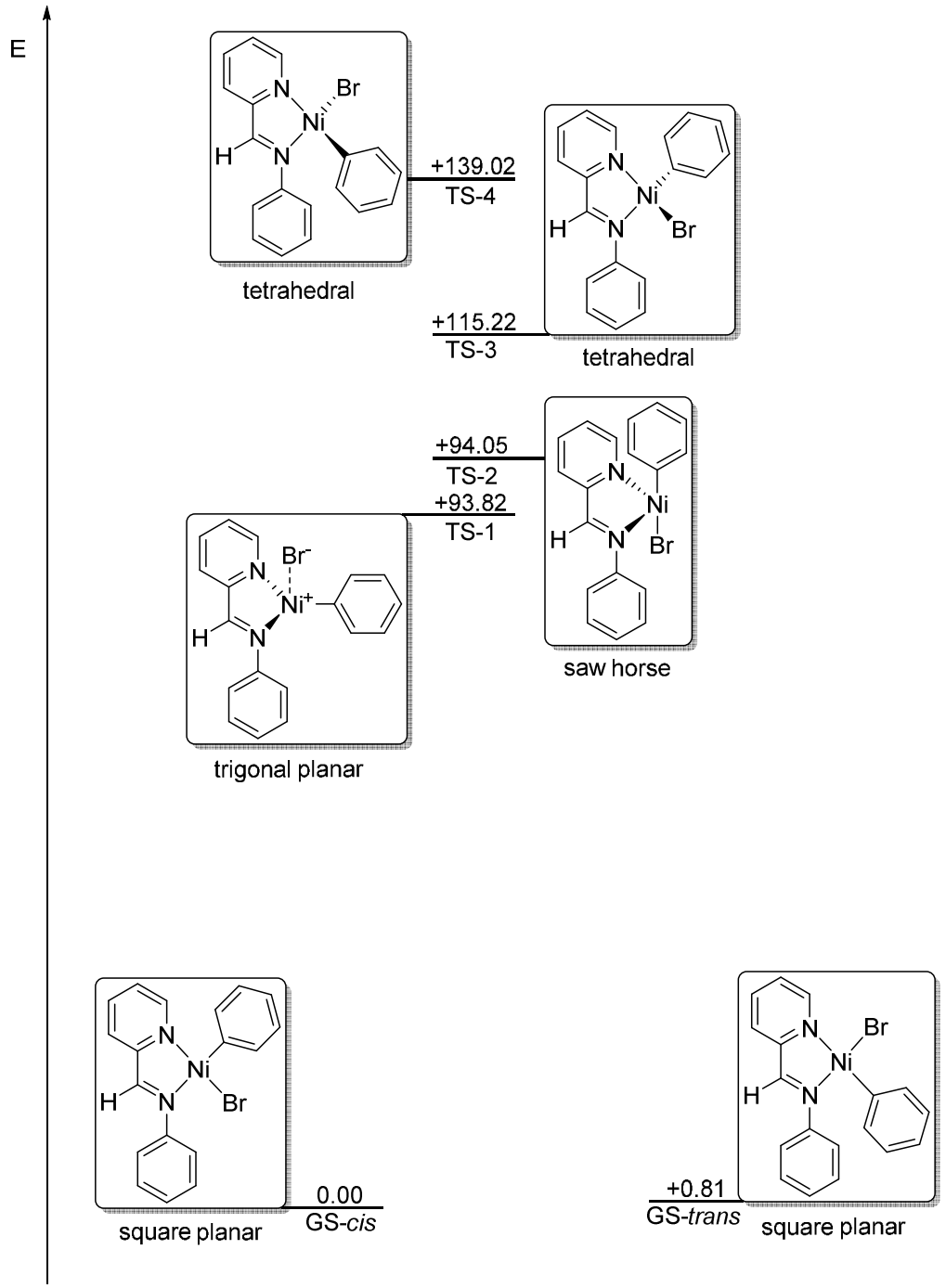

Figure S10: Calculated transition states during *cis-trans* isomerization of [(PyMA)Ni(Ph)Br].

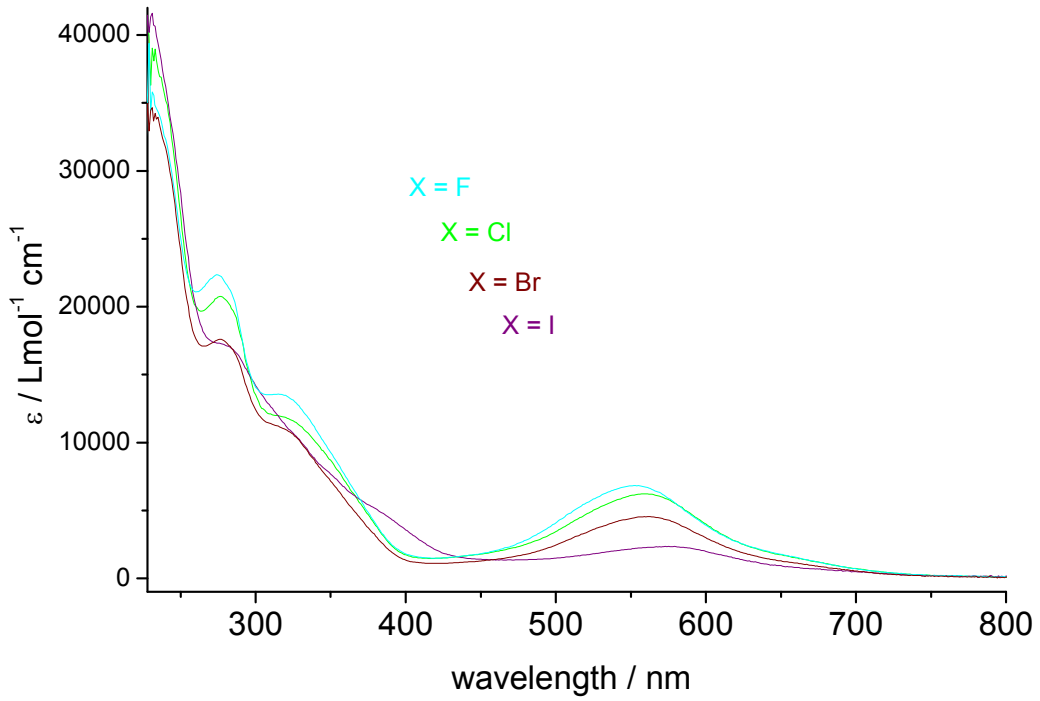

Figure S11: UV-vis absorption spectrum of [(PyMA)Ni(Mes)X] in CH_2Cl_2.

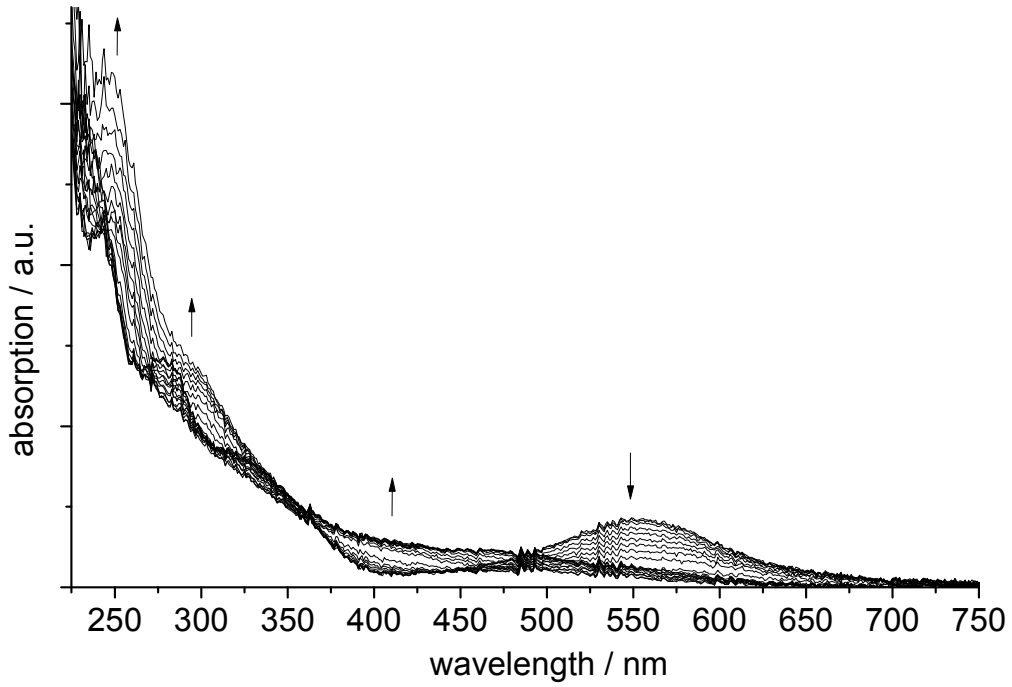

Figure S12: SEC UV-vis absorption spectra of [(PyMA)Ni(Mes)Br] during reductive electrolysis in THF/^{n}Bu$_4$NPF$_6$ solutions. The spectra represent potential differences of 0.01 V between –1.6 and –1.75 V vs. ferrocene/ferrocenium.

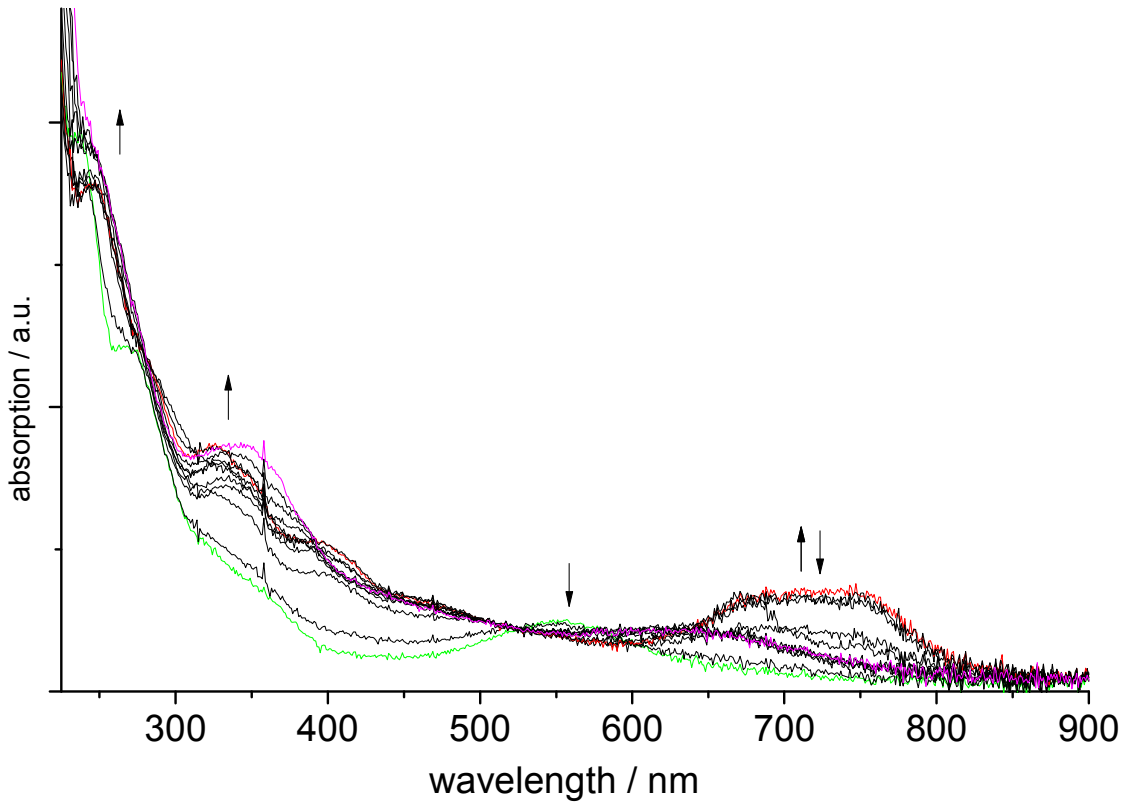

Figure S13: UV-vis absorption spectra of [(2NO_2-4Me-PyMA)Ni(Mes)Br] during reductive electrolysis in THF/^{n}Bu_4NPF_6 solutions. Green represents the parent complex, red the one-electron reduced species (NO_2 reduction) and magenta the two-electron reduced species.

D) Supporting Tables

Table S1: Selected crystal and structural refinement data for nickel complexes [a]

	Cis-[(PyMA)Ni(Mes)Cl]	*trans*-[(PyMA)Ni(Mes)Br]	*trans*-[(4-NO_2-PyMA)Ni(Mes)Br]	*trans*-[(3,5-Me_2-PyMa)Ni(Mes)Br]	*cis*-[(2-CF_3-PyMA)Ni(Mes)Br]	*cis*-[(2-NO_2-4Me-PyMA)Ni(Mes)Br]·CH_2Cl_2	*cis*-[(Mes-PyMA)Ni(Mes)Br]	*cis*-[(2,6-$^iPr_2$-PyMA)Ni(Mes)Br]
formula	$C_{21}H_{21}ClN_2Ni$	$C_{21}H_{21}BrN_2Ni$	$C_{21}H_{20}BrN_3NiO_2$	$C_{23}H_{25}BrN_2Ni$	$C_{44}H_{40}Br_2F_6N_4Ni_2$	$C_{22}H_{22}BrN_3O_2Ni{\bullet}CH_2Cl_2$	$C_{24}H_{27}BrN_2Ni$	$NiC_{27}H_{33}N_2Br$
weight /g·mol^{-1}	395.56	440.01	485.02	468.07	1016.04	583.97	482.08	524.17
T /K	293(2)	293(2)	293(2)	293(2)	293(2)	293(2)	293(2)	293(2)
crystal system	trigonal	monoclinic	monoclinic	monoclinic	triclinic	monoclinic	monoclinic	monoclinic
space group	*R*3c	$P2_1/c$	$P2_1/n$	$P2_1/c$	$P\bar{1}$	$P2_1/c$	*C*2/c	$P2_1/c$
a /Å	23.19(1)	15.83(1)	8.50(1)	8.72(1)	11.76(1)	12.53(1)	38.62(1)	10.83(1)
b /Å	23.19(1)	8.02(1)	15.45(1)	16.16(1)	13.38(1)	13.60(1)	8.11(1)	15.99(1)
c /Å	20.12(1)	15.21(1)	15.74(1)	15.60(1)	15.42(1)	14.75(1)	15.40(1)	14.45(1)
α /°	90	90	90	90	82.8(1)	90	90	90
β /°	90	93.9(1)	97.7(1)	104.6(1)	68.1(1)	96.0(1)	109.3(1)	90.8(1)
γ /°	120	90	90	90	78.7(1)	90	90	90
volume /Å^3; Z	9370(3); 18	1926.6(1); 4	2048.7(7); 4	2128.1(4); 4	2204.3(3); 2	2498.5(2); 4	4548.7(2); 8	2502.6(3); 4
density, calc. /g/cm^3	1.262	1.517	1.573	1.461	1.531	1.552	1.408	1.391
F (000)	3708	896	984	960	1024	1184	1984	1088
total reflections; unique reflections	36653; 4764	21632; 4083	19292; 4558	20355; 4522	33437; 9356	30702; 5315	13746; 4670	14505; 5575
*R*int	0.3782	0.1108	0.1334	0.3045	0.2132	0.0845	0.1915	0.1018
*R*1; *wR*2 [I_0>2σ(I)]	0.0704; 0.1602	0.0441; 0.1213	0.0454; 0.0606	0.0536; 0.0772	0.0463; 0.0531	0.0449; 0.1077	0.0819; 0.1518	0.0563; 0.1279
*R*1; *wR*2 [all data]	0.2137; 0.1937	0.0568; 0.1308	0.1714; 0.0822	0.2544; 0.1172	0.2666; 0.0892	0.0891; 0.1263	0.2145; 0.2011	0.1046; 0.1458
Goof on F^2	0.730	1.033	0.766	0.708	0.745	0.992	0.978	0.966
Residual /e·Å^{-3}	1.608; –0.473	1.302; –1.055	0.358; –0.291	0.358; –0.784	0.261; –0.483	0.694; –0.601	0.533; –0.660	1.717; –0.794
CCDC	1495248	1495249	1495250	1495251	1495252	1495253	1495254	1495255

[a] All samples measured at 293(2) K using Mo-Kα radiation (λ = 0.71073 Å) and employing ω-φ-2θ scan technique.

The solved crystal structures of *cis*-[(PyMA)Ni(Mes)Cl], *trans*-[(3,5-Me_2-PyMa)Ni(Mes)Br], and *cis*-[(2CF_3-PyMA)Ni(Mes)Br] are of quite low quality and level A alerts appeared in the checkCIF/PLATON reports. We re-checked the solutions once again without better results, thus the low quality is due to low quality of the diffracted crystals in addition to the measurement at 293(2) K.

Table S2: Selected bond lengths /Å and angles /° of nickel complexes.

bond lengths	*cis*-[(PyMA)Ni(Mes)Cl]	*trans*-[(PyMA)Ni(Mes)Br]	*trans*-[(4NO_2-PyMA)Ni(Mes)Br]	*trans*-[(3,5Me_2-PyMa)Ni(Mes)Br]	*cis*-[(2CF_3-PyMA)Ni(Mes)Br]	*cis*-[(2NO_2-4Me-PyMA)Ni(Mes)Br]·CH_2Cl_2	*cis*-[(Mes-PyMA)Ni(Mes)Br]	*cis*-[(2,6^iPr_2-PyMA)Ni(Mes)Br]
N1–Ni1	1.90(1)	1.99(1)	1.98(1)	1.99(1)	1.92(1)	1.91(1)	1.90(1)	1.92(1)
N2–Ni1	2.01(1)	1.91(1)	1.91(1)	1.94(1)	1.99(1)	2.00(1)	1.99(1)	1.99(1)
Ni1–X1	2.17(2)	2.29(1)	2.30(1)	2.30(1)	2.29(1)	2.30(1)	2.29(1)	2.31(1)
Ni1–C31	1.90(2)	1.89(1)	1.88(1)	1.90(1)	1.91(1)	1.89(1)	1.90(1)	1.91(1)
angles								
C31–Ni1–N2	171.3(7)	93.8(1)	93.1(2)	95.5(4)	175.3(4)	174.1(1)	172.8(1)	169.2(2)
N1–Ni1–X1	173.4(5)	96.84(9)	95.8(1)	94.8(1)	179.0(2)	174.9(1)	172.7(3)	169.3(2)
N2–Ni1–X1	97.4(4)	171.1(1)	173.3(1)	173.0(2)	96.2(2)	96.3(1)	96.3(2)	94.6(1)
X1–Ni1–C31	90.4(5)	88.4(1)	88.8(2)	87.6(3)	88.4(2)	89.5(1)	89.7(3)	91.3(1)
N1–Ni1–C31	91.2(6)	171.2(1)	175.1(2)	174.1(4)	92.6(3)	91.9(1)	92.7(4)	93.4(2)
N1–Ni1–N2	81.6(6)	82.2(1)	82.2(2)	82.7(3)	82.8(3)	82.5(1)	81.9(3)	82.4(1)
dihedral angles								
N1–Ni1–C31–C36	83.0(1)	84.9(3)	69.5(5)	76.6(8)	88.9(9)	85.9(3)	89.9(8)	79.0(4)
C1–N2–C11–C12	48.0(3)	65.3(5)	54.7(7)	52.0(1)	82.4(9)	55.0(2)	69.4(2)	89.0(5)
Sum of angles	360.6(1)	361.2(1)	361.2(1)	360.6	360(1)	360(1)	360.6(1)	361.7(1)

X = Cl or Br.

Table S3: Calculated energies for the *cis* and *trans* isomers of the complexes.

Complexes	*cis* [Hartree]	*trans* [Hartree]	E_{cis} - E_{trans} [Hartree]	E_{cis} - E_{trans} [kJ/mol]	pref. isomer
[(PyMA)Ni(Mes)Br]	-5005.90641962546	-5005.90543216875	-0.0009874567	-2.592567763341	*cis*
[(PyMA)Ni(Mes)I]	-2729.31859445117	-2729.31759393728	-0.0010005139	-2.626849444553	*cis*
[(PyMA)Ni(Mes)F]	-2531.32839019195	-2531.32632891235	-0.00206127960	-5.4118900020559	*cis*
[(PyMA)Ni(Mes)Cl]	-2891.72292817763	-2891.72181851225	-0.00110966538	-2.9134266771231	*cis*
[(3,5-$(OMe)_2$-PyMA)Ni(Mes)Br]	-5235.06087905626	-5235.06235208430	0.00147302804	3.8674354136256	*trans*
[(3,5-Me_2-PyMA)Ni(Mes)Br	-5084.569089529	-5084.56801112381	-0.00107840519	-2.831353042026	*cis*
[(4-NO_2-PyMA)Ni(Mes)Br]	-5210.53345759529	-5210.53221546176	-0.00124213353	-3.26122183144171	*cis*
[(2-NO_2-4-CH_3-PyMA)Ni(Mes)Br]	-5249.85656192252	-5249.85385502134	-0.00270690118	-7.1069695894702	*cis*
[(2-CF_3-PyMA)Ni(Mes)Br]	-5343.11337428239	-5343.11053051178	-0.00284377061	-7.46632030530912	*cis*
[(2-CF_3-6-F-PyMA)Ni(Mes)Br]	-5442.39775127780	-5442.39261420258	-0.00513707522	-13.487392017525	*cis*
[(Mes-PyMA)Ni(Mes)Br	-5123.89612353309	-5123.89012794725	-0.00599558584	-15.741411822037	*cis*
[(2,6-Me_2-PyMA)Ni(Mes)Br]	-5084.56515548442	-5084.55893699370	-0.00621849072	-16.3266486290581	*cis*
[(2,6-^{i}Pr_2-PyMA)Ni(Mes)Br]	-5241.86727889301	-5241.85808461587	-0.00919427714	-24.1395764699254	*cis*

Table S4: Absorption maxima of the complexes [(R-PyMA)Ni(Mes)Br] in CH_2Cl_2.[a]

R-PyMA	**$\lambda_1(\varepsilon)$**	**$\lambda_2(\varepsilon)$**	**$\lambda_3(\varepsilon)$**	**$\lambda_4(\varepsilon)$**
PyMA	239 (25.6)	278 (14.7)	324 (8.4)	570 (4.5)
3,5Me_2	240 (24.5)	272 (14.6)	317 (10.7)	559 (2.2)
Mes	238 (23.2)	278 (19.1)	364 (4.2)	548 (4.3)
2,6Me_2	236 (26.2)	278 (17.8)	362 (3.9)	551 (4.7)
2,6^iPr_2	237 (26.6)	276 (21.0)	361 (3.8)	552 (4.3)
2NO_2-4Me	241 (30.2)	272 (21.6)	323 (8.5)	562 (4.1)
4NO_2	238 (23.3)	286 (22.5)	344 (10.2)	574 (4.0)
3,5$(OMe)_2$	237 (40.0)	268 (25.1)	326 (10.1)	559 (2.6)
2CF_3	232 (40.3)	288 (24.1)	334 (7.2)	561 (2.9)
2CF_3-6F	235 (38.0)	272 (24.0)	332 (4.9)	564 (2.7)

[a] Wavelengths of absorption maxima λ in nm; molar absorption coefficient ε in 1000 $M^{-1}cm^{-1}$.

Table S5: Absorption maxima of [(PyMA)Ni(Mes)X] with X = F, Cl, Br, or I in various solvents.[a]

[(PyMA)Ni(Mes)X]	$\lambda_1(\varepsilon)$	$\lambda_2(\varepsilon)$	$\lambda_3(\varepsilon)$	$\lambda_4(\varepsilon)$	solvent
X = F	234 (34.8)	274 (22.6)	323 (13.4)	536 (7.1)	CH_2Cl_2
	239 (37.3)	281 (21.2)	326 (12.6)	533 (4.2)	THF
	237 (29.2)	280 (18.6)	330 (10.6)	514 (2.8)	acetone
X = Cl	233 (37.6)	275 (20.7)	326 (11.7)	553 (6.1)	CH_2Cl_2
	240 (40.3)	272 (22.6)	326 (12.3)	547 (8.1)	THF
	-	-	-	538 (9.5)	acetone
X = Br	239 (39.4)	277 (18.7)	324 (10.4)	570 (4.5)	CH_2Cl_2
	230 (38.4)	279 (17.4)	328 (9.6)	568 (4.6)	THF
	-	-	-	546 (6.0)	acetone
X = I	234 (40.8)	277 (17.2)	388 (5.1)	578 (2.1)	CH_2Cl_2

[a] Wavelengths of absorption maxima λ in nm; molar absorption coefficient ε in 1000 $M^{-1}cm^{-1}$.

Table S6: Selected UV-vis spectroelectrochemical data of parent and reduced complexes [(PyMA)Ni(Mes)Br], [(2NO_2-4Me-PyMA)Ni(Mes)Br] und [(3,5$(OMe)_2$-PyMA)Ni(Mes)Br].[a]

complex	absorption maxima parent compound	absorption maxima after reduction [b]
[(PyMA)Ni(Mes)Br]	230, 279, 328, 568	247, 303, 423
[(2NO_2-4Me-PyMA)Ni(Mes)Br]	238, 276, 366, 556	247, 342, 404, 715
[(3,5$(OMe)_2$-PyMA)Ni(Mes)Br]	227, 277, 345, 562	259, 295, 422

[a] Wavelengths of absorption maxima λ in nm. [b] Generated by *in situ* electrolysis in THF/0.1 M $^{n}Bu_4NPF_6$ at ambient temperatures.

Table S7: Catalytic cross-coupling tests of [(R-PyMA)Ni(Mes)X] complexes under Negishi conditions with the yield of hetero- and homo-coupling products.

products	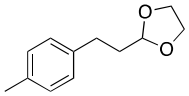	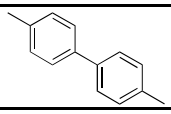	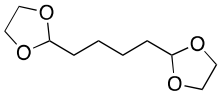
catalyst			
[(bpy)Ni(Mes)Br]	42.5%	-	-
[(PyMA)Ni(Mes)Cl]	32.6%	7.3%	17.8%
[(PyMA)NiMesBr]	21.4%	0.5%	1.7%
[(3,5-$(MeO)_2$-PyMA)Ni(Mes)Br]	11.0%	2.4%	13.5%
[(4-NO_2-PyMA)Ni(Mes)Br]	28.4%	8.2%	19.8%
[(Mes-PyMA)Ni(Mes)Br]	24.3%	3.7%	7.1%
[(2-NO_2-4-Me-PyMA)Ni(Mes)Br]	18.8%	3.4%	20.8%
products	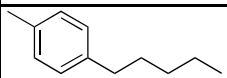	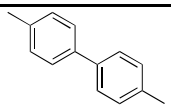	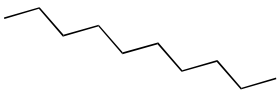
catalyst			
[(bpy)Ni(Mes)Br]	100%	-	-
[(PyMA)Ni(Mes)F]	18.7%	6.9%	16.3%
[(PyMA)Ni(Mes)Cl]	26.5%	10.3%	29.4%
[(PyMA)NiMesBr]	65.3%	2.2%	8.2%
[(3,5-$(MeO)_2$-PyMA)Ni(Mes)Br]	19.3%	8.6%	11.9%
[(4-NO_2-PyMA)Ni(Mes)Br]	34.9%	6.8%	46.8%
[(Mes-PyMA)Ni(Mes)Br]	49.4%	5.3%	30.3%
[(2-NO_2-4-Me-PyMA)Ni(Mes)Br]	31.0%	5.4%	30.2%